

# **ANALYSIS OF SINGLE-PHASE TRANSFORMER LESS INVERTER FOR HYBRID RENEWABLE ENERGY SOURCES**

**K.TEJA SREE<sup>1</sup>, B. RAJESH<sup>2</sup>**

<sup>1</sup>PG scholar, Department of Electrical and Electronics Engineering Vidya Jyothi Institute of Technology Aziz Nagar Gate, C.B. Post, Hyderabad-75

<sup>2</sup>Assistant Professor, Department of Electrical and Electronics Engineering Vidya Jyothi Institute of Technology Aziz Nagar Gate, C.B. Post, Hyderabad-75

## **Abstract**

Solar and wind energy are not depleted natural resources that are more popular and popular. Solar and wind power as alternative energy sources can be accessed and easily obtained. Solar and wind energy combined with the Solar Wind Hybrid Power System (SWHPS), which increases each other's qualities. The optimized use of these natural resources is essential to generate power, in order to reduce the demand for power in the conventional energy sector. Specific techniques are generally used for power generation using the Solar Wind Hybrid System (MPP). A proportional resonant control technique is used to regulate the injected current. A high voltage system is used to monitor the injected power transfer. A key advantages of the inverter proposed are: (1) Grid neutral was directly connected to negative terminal of panel to remove leakage current; 2) it is compact size; 3 ) low price; 4) inverter's used in dc voltage is same as that of full-bridge inverter. Here operating principle is described in detail and inverter analysis is presented.

**Key words:** Solar Wind Hybrid Power System (SWHPS), Transformer less inverter, leakage current.

## **I. INTRODUCTION**

Photovoltaic energy systems have become a popular power system among renewable sources over a last two decades because of an absence of moving parts and a quiet working conditions without emissions and low maintenance requirements [2]. As an integral part of a power grid, distributed grid connected PVs play an ever more important role. PV systems suffer from a high common mode current because of a large stray condensers between a PV panels and a ground that reduce system efficiency and can lead to security problems like an electric shock. Transformers in a PV network are typically used to provide galvanic isolation to remove a leakage currents. It has unnecessary properties, including large sizes, high cost and potential weight losses [3]. Eliminating a transformer therefore represents a significant advantage in further enhancing system efficiency, a size and weight of a system [4]. One of an important issues for PV applications connected to a transformer less grid is galvanic grid and PV network link, leading to problems with current leakage. a proposed reduction in a drainage current by disconnecting a grid from a PV during freewheeling modes[6] was proposed for inverters attachment to a transformer less grid by Fiel Bridge (FB), Neutral Point Clamped (NPC), Active NPC (ANPC) [5] and several other topologies, such as H5, H6 and HERIC. Such topologies, however, are not totally free from a current or leakage of can mode (CM). Owing to a parasite condenser of a switch and a stray power between a PV and a field, a leakage current still exists. Some of these topologies therefore require two or more filter inductors to reduce a leakage current, resulting in an increase in system volume and cost [7]. Picture. 1 illustrates a single-phase grid with a CM current path tied transformer less inverter, where P and N are respectively positive and negative PV terminals.

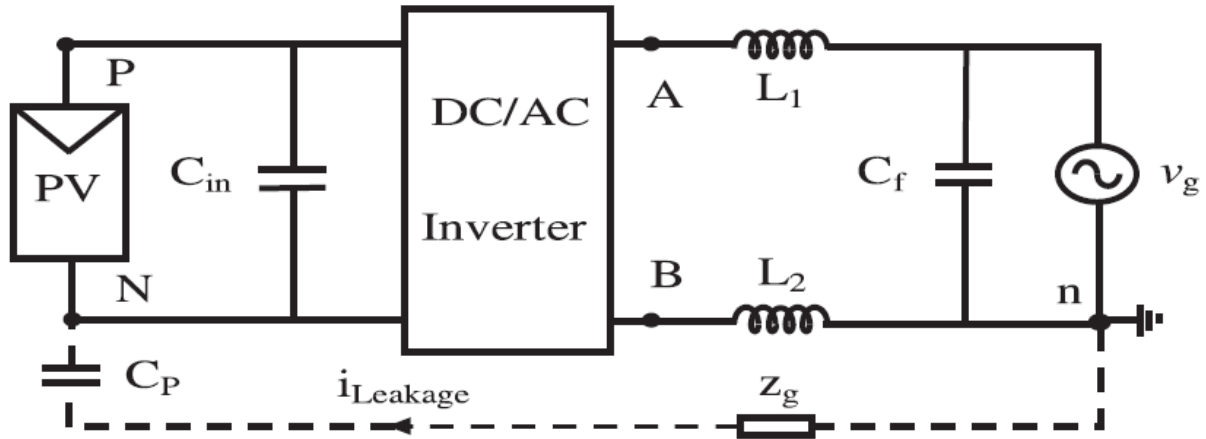


**Fig. 1 Single-phase grid connected transformer-less inverter with a leakage current path.**

The leakage current ( $i_{Leakage}$ ) flows through ( $L_1$  and  $L_2$ ) filters, inverters, gate and earth impedances ( $Z_g$ ) through a parasitic condenser ( $C_p$ ). Leak current can cause safety difficulties, reduce injection current quality to the grid and reduce an efficiency of system [8]. Common Mode Voltage (CMV) ( $V_{cm}$ ) must be maintained constant in all operating modes according [9] in order to eliminate the leakage capacity.  $V_{cm}$  is measured using two filter inductors ( $L_1, L_2$ ) as:

$$v_{cm} = \frac{V_{An} + V_{Bn}}{2} + \frac{(V_{An} - V_{Bn})(L_2 - L_1)}{2(L_1 + L_2)} \dots\dots(1)$$

Where  $v_{An}$  and  $v_{Bn}$  are the variations in voltage between inverter midpoint A and midpoint B in dc bus minus terminal N. When the  $v_{cm}$  is calculated according to (1) for  $L_1 \neq L_2$  asymmetric inductors and leakage current appears because of a different CMV. When the  $v_{cm}$  ( $L_1 = L_2$ ) is simplified: If the  $v_{cm}$  is:

$$v_{cm} = \frac{V_{An} + V_{Bn}}{2} = const.. \dots\dots(2)$$

The usual mode voltage in this state shall be constant and the leakage current shall be removed. One of the filter inductors is zero in some structures such as the virtual dc bus inverter [10] and NPC inverter and only one filter inductor is used. It will be constant according to (2) after simplification of  $v_{cm}$  and the leakage current is removed. As Fig 2, shows numerous grid-connected transformer-free inverters are specified on basis of FB inverter to address these problems.

$$v_{cm} = \frac{V_{An} + V_{Bn}}{2} + \frac{(V_{An} - V_{Bn})}{2} = const.. \text{if } (L_1 = 0) \dots\dots(3)$$

$$v_{cm} = \frac{V_{An} + V_{Bn}}{2} - \frac{(V_{An} - V_{Bn})}{2} = const.. \text{if } (L_2 = 0) \dots\dots(4)$$

Compared to traditional FB inverters, a H5 inverter requires an additional switch ( $S_5$ ) on a dc side to isolate a dc side from a grid, as shown in a figure. 2(a) A variable CM voltage of this inverter is small in leakage and low in efficiency due to an operation of three switches at a same time [11]. As Fig shows. 2(b), HERIC's topology requires two additional switches to decouple an ac side from a PV module in a nil stage. An ac side must be cut off from a PV module at nil level. HERIC combines unipolar and bipolar modulation advantages. A HERIC inverter has main advantage because only two switches operate simultaneously in all operating modes. HERIC topology's main drawbacks are a low-frequency harmonics and reactive power flows are not permitted [12]. H6-based topologies are also proposed to eliminate a grid-bound PV application leakage current in [13] [14]. Six power switches and diodes are used to disconnect a dc side from a grid.

These topologies are more expensive than a FB inverter since extra switches and diodes are used. Another drawback of these topologies is lower efficiency because of a current circulating simultaneously through three power switches [15]. Several highly efficient new H6 transformer-free inverters are proposed for light weight and lower cost in [16] and [17] respectively. They are able to inject reactive power into a grid. In these topologies, which is a main disadvantage of a leakage current is not entirely eliminated. A direct link of a negative PV terminal to a grid neutral

point, for example a virtual dc bus inverter in [10] and an unusual topology in [18], are another solution for removal of a leakage current. A leakage current is removed completely through a topology structure in these topologies. As Fig shows. In 2(c), an inverter for an essentially dc bus consists of five IGBTs, two condensers and one LF filter. In this topology, only one filter inductor is used to remove a leakage current. A virtual dc bus produces a negative voltage output. A biggest downside of this topology is that during a negative process there's no way to charge a C2 condenser and that's high THD performance. In [18], a topology is shown in a figure. 1.2(d) has a grid base in common. This topology has a low semi-conductor number. However, this inverter only has a two-tier output voltage, including a positive and negative voltage, without a zero voltage generating a large L2, and a filter output. Another topology that is derived from buck-boost topology is an inductor medium type inverter [19] also called "Karschny." Without reactive power to a grid, an inverter has a high reliability and has four power switches on a current path, which reduces efficiencies.

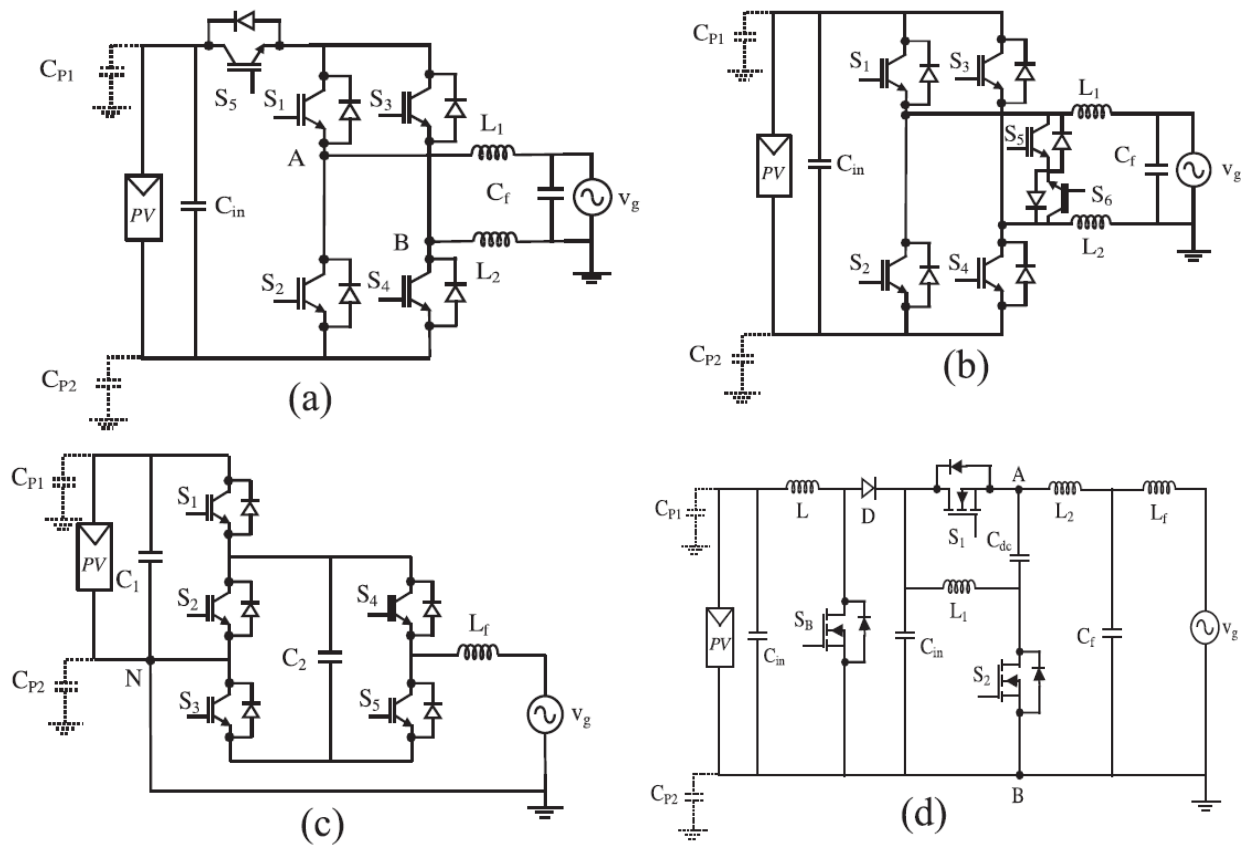


**Fig. 2. PV inverter topologies of Single phase grid tied transformer-less: (a) H5 inverter (b) HERIC inverter (c) virtual dc bus inverter [10] (d) common mode inverter proposed in [18].**

In this paper, a new transformer-less inverter is introduced based on a charging pump circuit concept. A PV systems with unipolar sinusoidal pulse width (SPWM) method eliminates leakage current in grid connected systems. This solution directly connects a neutral grid of a recharge pump system to a negative terminal, thereby eliminating a leakage current by connecting a voltage across a parasite condenser to 0. To produce negative output voltage, a charging pump circuit is implemented. A modulation of a proposed inverter is not limited because a circuit topology eliminates a current of a leakage. A suggested topology consists of only four power switches, which decreases a cost of semiconductors and increases a power quality by three-story power output voltage to minimize a current output shock. A current flows through two switches during an operation of a proposed inverter; a lead loss is therefore smaller. In contrast to NPC, ANPC and half-bridge (HB) inverters, a usual dc voltage of a proposed inverter is a same as a FB inverter. A proposed reactive power inverter can also be supplied to a grid.

## II. LITERATURE SURVEY

### **Recent advances in single-phase transformer-less photovoltaic inverters**

There has been a steady increase in renewable energy generation in recent years. In particular, because of a possibility of installing low-energy plants that are easily integrated into urban environments, a domestic PV, a biggest increase has been recorded for grid-connected household energy production. According to this trend, in recent years academic and industrial research has spread significantly in order to maximize efficiency and reliability, by new solutions for grid-connecting single-phase inverters. Many innovations have already begun to slip onto a market. Initially, a line frequency transformer was designed to facilitate a design by establishing a galvanic isolation between a source of PV and a grid of a grid. However, a line transformer is a big part and a source of additional expense and power losses. A typical efficiency of such systems is less than 97%. An intermediate solution is a use of high frequency transformers that reduce a problem of a power density due to a reduced size of a magnetic core and retain an advantages of galvanic isolation. Anyway, a use of high frequency transformers necessarily increases a number and complexity of an inverter by modulating a DC power from a panels at high frequency, then converting it into a line frequency. There is a significant effect on an overall output that can be accomplished through a number of power steps and a dimensional constraints of a high Frequency Transformer (which eventually restricts a wiring parts, thus increasing a resistance). For all an above factors, transformers of PV plants of domestic scale were almost uniformly removed. Nowadays an efficient grid-connected converters on a market are transformer-free, with some companies claiming efficiencies of over 98 percent for their products. A use in grid-connected systems of transformer less inverters is nevertheless not easy. A lack of galvanic separation, such as ground flow currents and a risk of injecting DC power into a Grid, causes new issues. Many classifications have been suggested for single-phase transformer inverters over a past few years.

### **Evaluation and analysis of transformer-less photovoltaic inverter topology for efficiency improvement and reduction of leakage current**

Many inverter topologies have been proposed with grid-connected transformer-less photovoltaic (PV) inverter applications to reduce leakage current and to enhance performance. This study evaluates and analyzes a method to increase efficiency and reduce leakage current. In order to quantify switching losses, conduction losses and free-riding losses an operation of transformer-less PV inverters with high-performance topologies such as full-bridges, H5, H6, HERIC and parallel-buck topology is examined. Total device losses are calculated by switching frequency and an output power for inverter topology. In addition, a leg voltage and high-frequency equivalent circuit are proposed as a novel high frequency configuration of an inverter topology. In a proposed high frequency model, a relation between a parasitized condenser and its leakage current can be explained. A voltage magnitude in a parasite condenser is also derived mathematically. Efficiency of a multiple inverter topology is compared with output power, and a novel high frequency model analyzes a leakage current.

### **The Active NPC Converter and Its Loss-Balancing Control**

The topology was a simple solution for extending current two-tier VSC technology voltages and power rates that were severely constrained by blocking tensions of power semiconductors with active turning and switching capability. Therefore for medium-voltage applications, a converter is especially important (2.3 – 7.2 kV). Leading manufacturers were soon to launch a NPC VSC on a market and become ever greater [3]. It is currently commonly used for medium-voltage (MVD 'S), marine machinery, mining and traction applications for industry (e.g. rolling mills, fans, pumps and conveyors). New potential technologies are available on an emerging wind energy market. Recent studies have shown that for low voltage applications, NPC VSC is also a viable option, albeit for different reasons [5]. Figure demonstrates a topology. 1. A NPC-VSC provides two additional diodes per phase leg compared to a two-level converter with a direct series connection of devices. Such diodes link an "indirect-serial connection" point of a key switches to a converter's neutral point. This makes it possible to link a phase output to a neutral point of a converter and allows a topologies to be at three stages.

### **Leakage Current Analytical Model and Application in Single-Phase Transformer less Photovoltaic Grid-Connected Inverter**

The low-cost and high-efficiency characteristics make a grid-connected transformer less inverters (PV) popular for a use of residential solar generation systems. Sadly, a leakage current between a PV array and a ground is harmful through a stray condensers. This paper focuses on a method of suppressing current leakage, which considers all common-mode routes. A first is to develop an analytical model of a common fashion at switching frequency, which summarizes a rules on a removal of a frequency switching source. A new full-bridge-type conversion system and a compensation strategy for a half-bridge-type inverters have been finally proposed, based on existing models and guidelines. A current full bridge- and semi-bridge-type converters.

**Leakage Current Elimination of Four-Leg Inverter for Transformer less Three-Phase PV Systems**

Leakage elimination is one of a big problems for three-phase transformer photovoltaic (PV) systems. In this article, a three-phase four-leg PV inverter has been studied to eliminate a leakage current. A mechanism of generating a leakage current is clearly defined with a common mode loop model. Various typical modulating methods based on a carrier are discussed and their corresponding common mode voltages. To achieve a constant common mode voltage for a leakage current reduction, a new modulation strategy with a Boolean logic function is proposed.

**III. EXISITNG SYSTEM**

Fig . 3 Indicates the inverter associated with the proposed transformer-less grid. Total PV, wind, boost, transformer-free inverter and grid are included in the system. This system's key downside is the development of wafts.

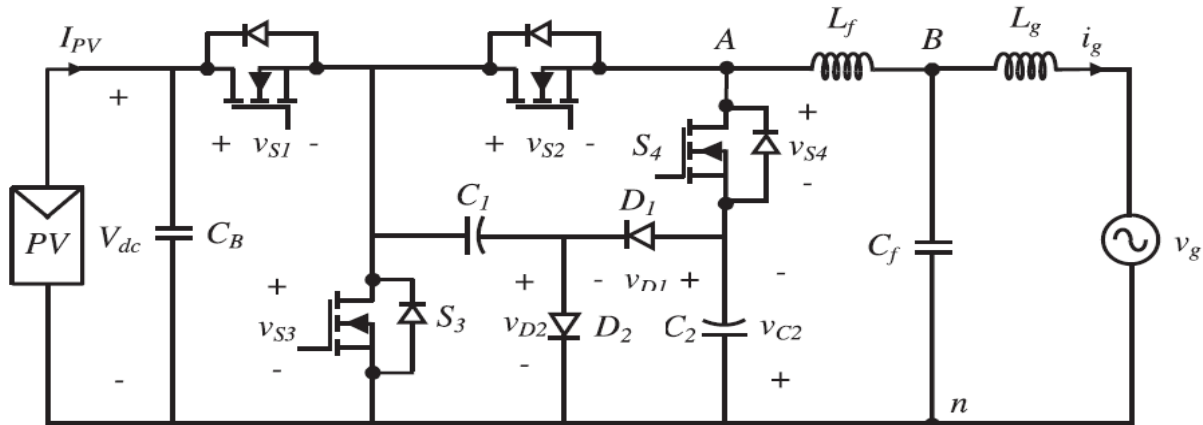


**Fig.3existing transformer-less grid associated inverter.**

**IV. PROPOSED SYSTEM**

Fig.4 shows the inverter associated with the planned transformer-less grid. Total PV, wind, boost, transformer-free inverter and grid are included in the system. As shown in figure, the proposed circuit comprises 2 diodes, 2 condensers&4 switches. DC-DC converters are supplied via a variable DC source, i.e. PV and WIND. DC-DC converters are supplied. The primary purpose of the boost converter is to transform variable dc to constant dc. The suggested inverter is supplied. The hysteresis controller controls this inverter. Rib-free ac to grid is provided to the output of the proposed inverter. The complete scheme as shown below. The entire scheme.

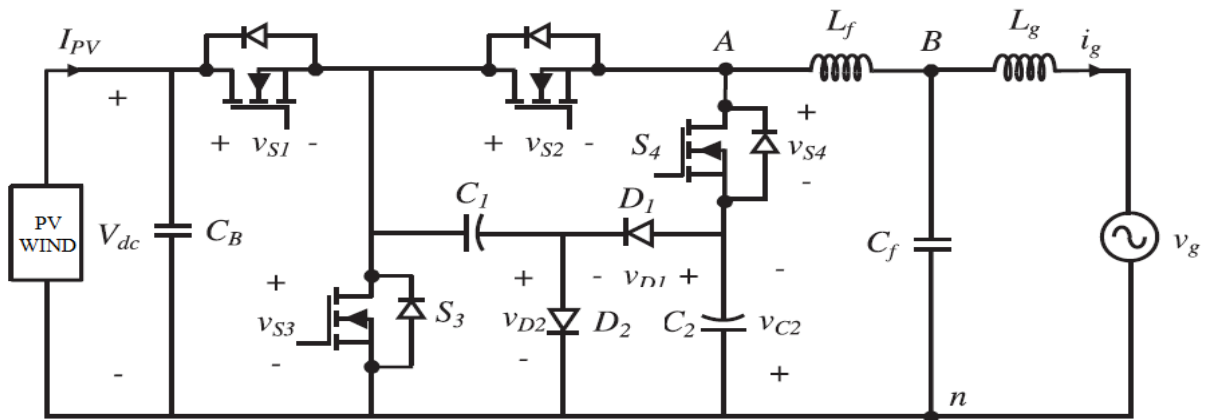


**Fig.4 Proposed transformer-less grid associated inverter.**

**PV PANEL WITH MPPT:**

In this paper, P&O MPPT technique victimization DC-DC Boost is followed through a versatility generation of a stand. That zone unit fed to a MPPT law, which in effect generates a job size relationship in line with variations in voltage and power. First, a voltage and current merchandise is completed to generate electricity. A distinction between flexibility and previous values, i.e. a distinction between  $P_{old} - P_{new}$  is calculated. Similarly,  $V_{old} - V_{new}$  also measures a difference in voltage. In an event of positive power adjustment and negative voltage changes, a process is shown on a left side of a plug in a Figure at intervals. 6.3 MPPT laws adjust a boost device's duty magnitude ratio to raise a panel operating voltage. A power supply will increase as shown below by increasing an operating voltage. In a same way, if an operating purpose for most wall plug is correct, a MPPT rule changes a boost converter duty relationship to chop an operating voltage of a PV panel. A steps of an algorithm. It is a P&O rule that is to start so-called "hill-climbing," but each name depends on that with a constant rule. Climbing requires a disturbance of a power converter's operating cycle and P&O disturbance of an operating voltage of a DC link between a PV array and a plant converter. Among a Hill climbing cases, a worrisome power converter duty cycle involves changing a DC connection voltage between a PV array and a facilities converter, so that each name refers to a continuously technical situation. A last change is marked in this system and a last rise between a measuring units used is marked together.

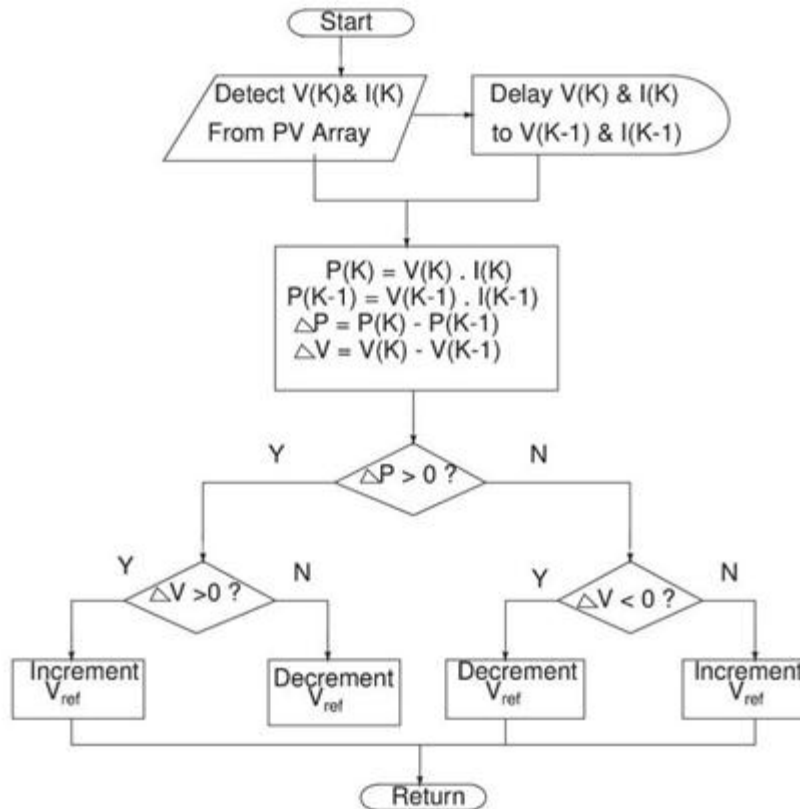


**Fig 5 P&O MPPT algorithm**

**WIND SYSTEM**

The turbine is a PMDC turbine in the wind network. The wind turbine with generator is shown in Figure 2 below. The PMDCG rotating torque is produced by the wind turbine. SFIG and DFIG are commonly used because they induce the voltage exchange as output. But the PMDC generator in this paper is used for DC output requests.

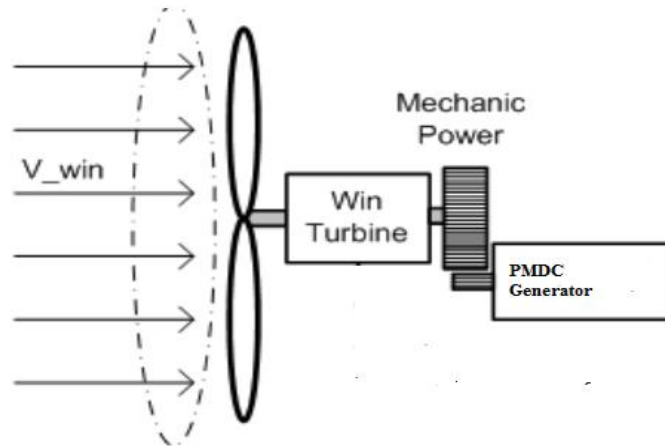


**Fig 6 wind turbine with PMDC generator**

**V. PROPOSED CONTROLLER FOR BIDIRECTIONAL POWERFLOW**

A physical phenomena controller is used to modify the controller and stabilize the system during the mode transitions. If current is positive in corrective mode, a single quadrangle calculation of the entire potential unit seconds applies to the inductance L1:

A1 will be used by DA2 in carrying out positive streams, and the management performance for DA2 will also be used for DA1 in carrying out positive streams. Under each corrective and electrical converter mode, one controller is often used to regulate current.

$$P = \frac{v_{g\alpha} i_{g\alpha} + v_{g\beta} i_{g\beta}}{2} \dots\dots(5)$$

$$Q = \frac{v_{g\alpha} i_{g\alpha} - v_{g\beta} i_{g\beta}}{2} \dots\dots(6)$$

where  $v_{g\alpha}$ ,  $v_{g\beta}$ ,  $i_{g\alpha}$ , and  $i_{g\beta}$  are the  $\alpha$  and  $\beta$  components of grid voltage and current, respectively. The active power and reactive power references ( $P^*$  and  $Q^*$ ) can be tuned by the operators  $\{R- 3\}$  or in the control unit, when the MPPT control is activated. The current reference can be computed in the  $\alpha\beta$ -reference frame, which simplifies the overall control. If PI controllers are used for power regulations, the grid current reference ( $i_{g-ref}$ ) can be derived as follows [14]:

$$i_{g-ref} = \frac{1}{v_{g\alpha}^2 + v_{g\beta}^2} [v_{g\alpha} \ v_{g\beta}] \begin{bmatrix} G_p(s) (P - P^*) \\ G_q(s) (Q - Q^*) \end{bmatrix} \dots\dots(7)$$

where  $G_p(s)$  and  $G_q(s)$  are the PI controllers for active power and reactive power, respectively.

The LCL filter is adopted as the grid interfaced filter in this proposed topology. High output current quality in the proposed inverter can be obtained if the output filter is configured correctly. The first design consideration is the calculation of the filter parameters, which can be determined by current ripple and filter values [25]. The inverter-side inductor ( $L_f$ ) value is calculated by considering 10–20% of the ripple on the output current, which is given by

$$L_f = \frac{(v_{dc} - v_{An})(M \sin \omega t)}{f_{sw} \Delta i_L} \dots\dots(8)$$

where  $f_{sw}$  is the switching frequency and  $\Delta i_L$  represents the peak-to-peak ripple current on the  $L_f$ . The inverter output voltage ( $v_{An}$ ) can be calculated as follows:

$$v_{An} = M V_{dc} \sin \omega t. \dots\dots(9)$$

By replacing (9) with (8) and simplifying it, we have

$$L_f = \frac{(v_{dc})(RF)}{f_{sw} \Delta i_L} \dots\dots(10)$$

where  $RF$  is the ripple current and can be calculated from

$$RF = M \sin \omega t - M^2 \sin^2 \omega t. \dots\dots(11)$$

The maximum achievable value of modulation index ( $M$ ) is  $RF_{max} = 0.25$  [26]. The maximum value of the filter capacitor is calculated by (42), limiting to be less than 5% of the nominal value [27]

$$C_{f,max} = \frac{0.05P_n}{2\pi f V_{rms}^2} \dots\dots(12)$$

where  $P_n$  is the nominal power,  $V_{rms}$  denotes the root mean square (RMS) grid voltage, and  $f$  presents the grid frequency. There is a relation between the inverter-side inductor ( $L_f$ ) and the grid side ( $L_g$ ). This value is determined with the ratio between the ripple attenuation ( $r$ ) as described in [28]

$$L_g = rL_f. \dots\dots(13)$$

The grid-side inductor ( $L_g$ ) value can be determined by

$$10f \leq f_{res} \leq 0.5f_{sw} \dots\dots(14)$$

The resonant frequency for the  $LCL$  filter is given by

$$f_{res} = (1/2\pi) \sqrt{(L_f + L_g)/L_f L_g C_f} \dots\dots(15)$$

Picture. Five displays the entire circuit diagram which contains a current loop management physical phenomenon. The current  $i_{ref}$  command is obtained by  $p_{ref}$  and  $Q_{ref}$  reactive power commands. The active and reactive power control is often used to calculate  $I$  and  $T$ , as illustrated below.

$$I_m = \left( \frac{P_{ref} + Q_{ref}}{\frac{V_{pk}}{2}} \right) \dots\dots(16)$$

$$\theta = \tan^{-1}(Q_{ref} + P_{ref}) \dots\dots(17)$$

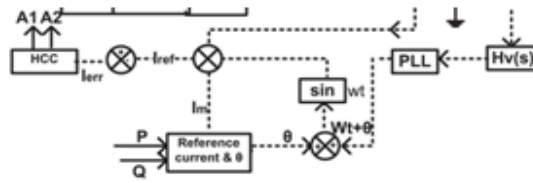


**Fig 7 Proposed hysteresis controller**

The voltage detector gain is from Fig.7  $H_v(s)$ , which is able to compare voltage input from the grid. The angle of voltage ( $\theta$ ) of the grid is given by PLL. Adding a dial to a clock produces current wave form reference. The error pulses zone unit created by natural phenomenon current controller A1 and A2 has been compared with the injected current  $i_{ac}$ . It generates  $i_{ref}$  partly during the vacation with grid voltage by giving exclusively + Pref input to the controller. If we've been bent on providing negative active power, the AC-DC system operates in a converter, pref and  $i_{ref}$  has a half distinction between 1800 and holiday making it work as a rectifier. Highly when active power Pref's zero, and reactive power Qref 's value as controller input, it will generate  $i_{ref}$  with an output of 90 degrees of half shift. 1800 half distinction with a grid voltage, and  $i_{ref}$  is comparable to a natural current controller relay (HCC) at all times, and the error is therefore supplied. If the error is negative, A1 switch is turned on to zero.5 negative voltage loop. A1 is turned OFF if the error is positive. A2 and D2 can operate in a positive zero.5 voltage loop. The controller generates  $i_{ref}$  with half shift with grid voltage, with instant  $i_{ref}$  comparable with  $i_{ref}$  at all times, in the case of the converter mode and therefore, the error produced is fed to the naturally occurring phenomenon controller relay (HCC). If the error is negative, the A2 switch will be turned on by the negative zero.5 voltage loop. A2 will be switched on if it is positive. A1 and D1 will function in a positive zero.5 loop.

**VI. SIMULATION RESULTS**

**PROPOSED SIMULATION RESULTS WITH HYBRID SYSTEM**

The proposed network diagram, consisting of PV, DC-DC converter, less inverter transformer and grid, should appear in Fig.8 indicates. The hysteresis controller interface displays in Fig.9

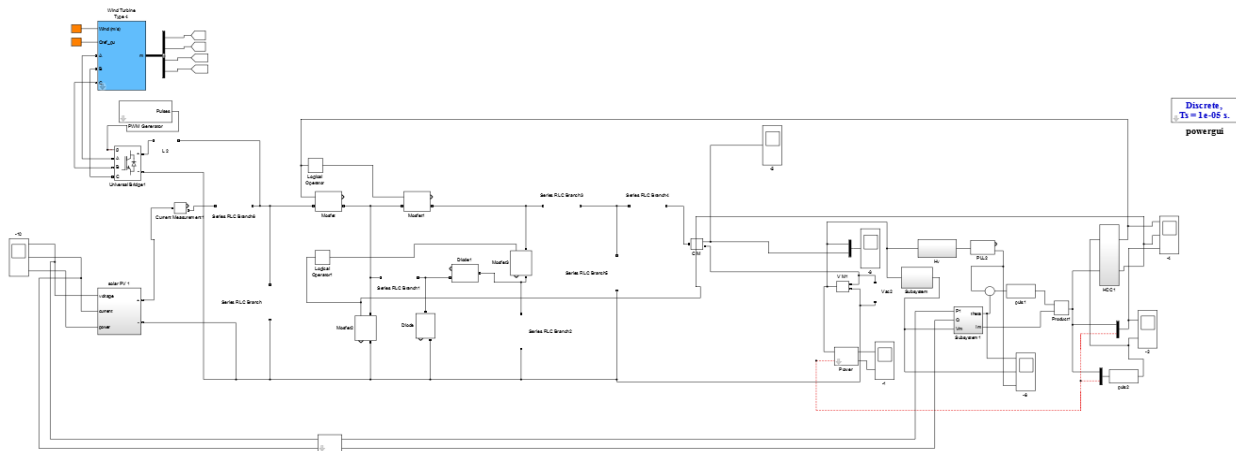


**Fig.8 MATLAB/SIMULINK diagram of proposed system with wind**

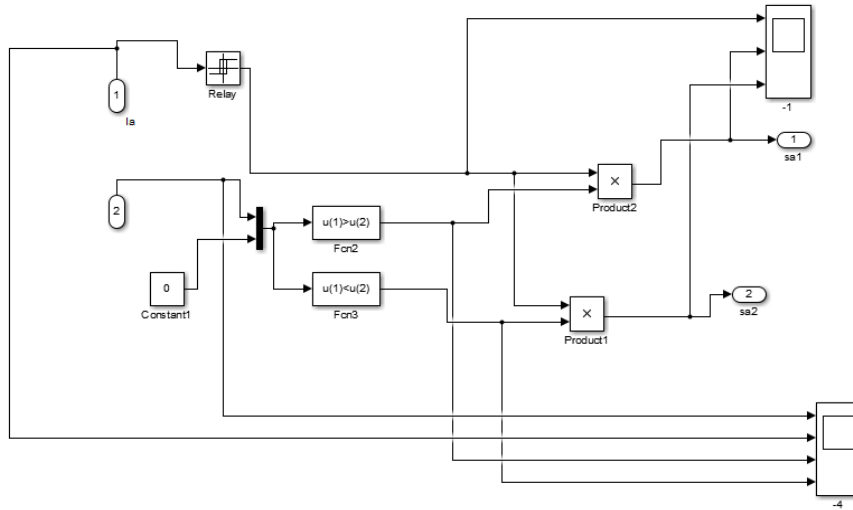


**Fig.9 Controller subsystem**

The input tension is shown in Fig.10, fig.11 shows output tension, fig.12 shows output tension. fig.13 indicates percentage of the THD tension present. The comparison of device voltages as described and proposed.

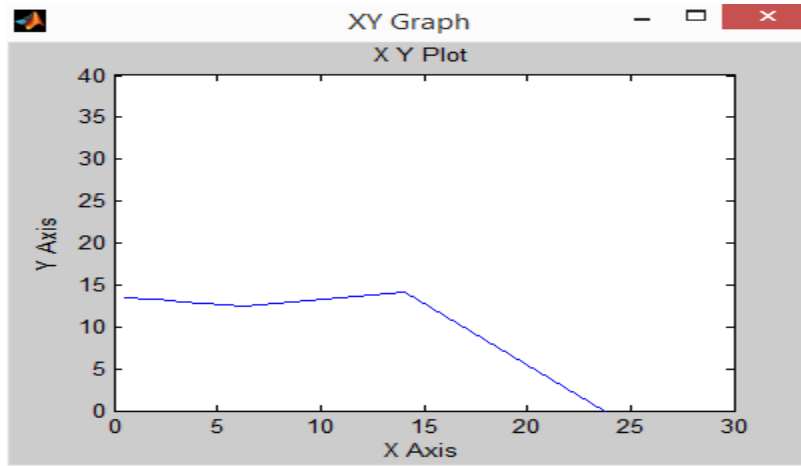


**Fig.10 Input waveform**

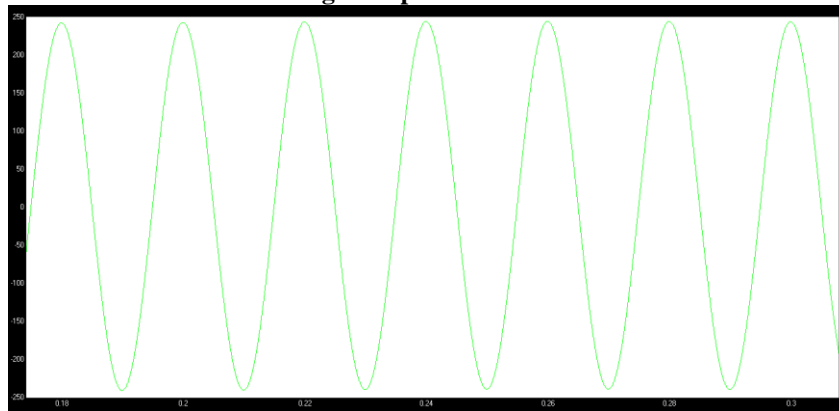


**Fig.11 Output Current**

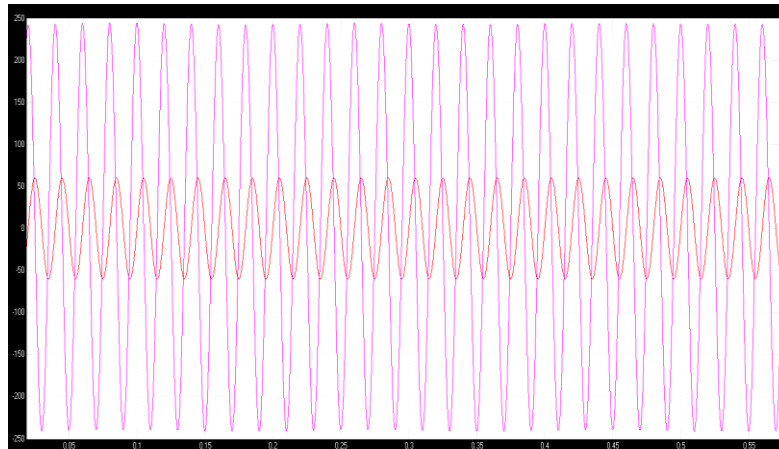


**Fig.12 Output Voltage**

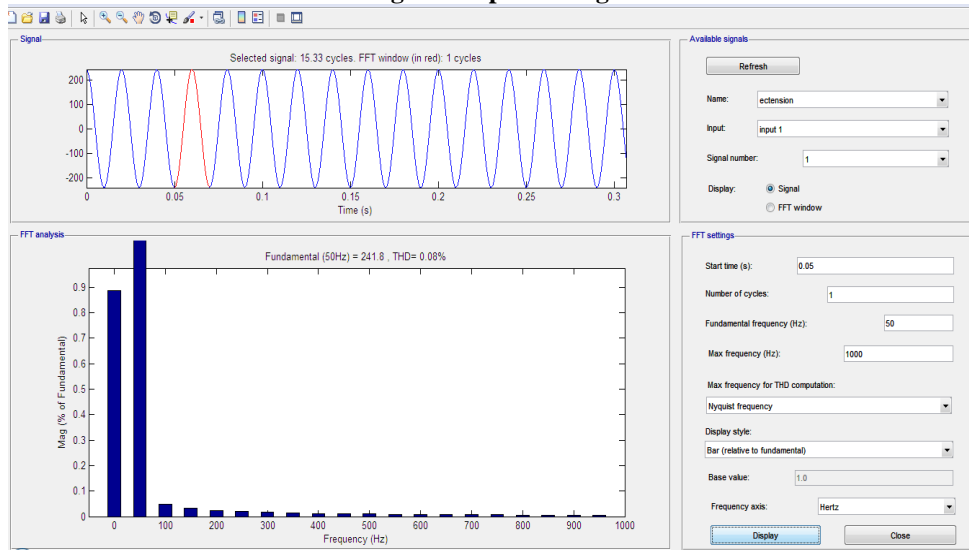


**Fig.13 THD% of voltage**

**COMPARISION RESULTS (THD)**

<b>BASE PAPER</b>	<b>EXTENSION</b>
<b>2.25%</b>	<b>0.08%</b>

**CONCLSION**

This article planned to use the loading pump circuit plan for a replacement one-stop device with less converser for a grid hybrid system (PV, WIND). The concept is designed to induce the planned converter with negative output voltage. A three-tier output voltage is generated by this new topology. As a consequence of a neutral line between the grids, the negative terminal of the expected topology is that the outpouring current is thus well super smooth and the system is removed additionally. Compact size, rising THD per cent, higher density and lower construction costs are the key advantages of a proposed network. The statute defined by the proposed inverter is highly efficient in comparison to other remaining transformer-less topologies. An analysis performed with the MATLAB simulation.

**REFERENCES**

- [1] S.B.Kjaer, J.K. Pedersen, and F.Blaabjerg, "A review of single-phase grid connected inverters for photovoltaic modules," *IEEE Trans. Ind. Electron.*, vol. 41, no. 5, pp. 1292–1306, Sep./Oct. 2005.
- [2] X. Guo, R. He, J. Jian, Z. Lu, X. Sun, and J. M. Guerrero, "Leakage current elimination of four-leg inverter for transformerless three-phase PV systems," *IEEE Trans. Power Electron.*, vol. 31, no. 3, pp. 1841–1846, Mar. 2016.
- [3] W.-J. Cha, K.-T. Kim, Y.-W. Cho, S.-H. Lee, and B.-H. Kwon, "Evaluation and analysis of transformerless photovoltaic inverter topology for efficiency improvement and reduction of leakage current," *IET Power Electron.*, vol. 8, no. 2, pp. 255–267, 2015.
- [4] H. Xiao and S. Xie, "Leakage current analytical model and application in single-phase transformerless photovoltaic grid-connected inverter," *IEEE Trans. Electromagn. Compat.*, vol. 52, no. 4, pp. 902–913, Nov. 2010.
- [5] T. Brückner, S. Bernet, and H. Guldner, "The active NPC converter and its loss-balancing control," *IEEE Trans. Ind. Electron.*, vol. 52, no. 3, pp. 855–868, Jun. 2005.
- [6] D. Barater, E. Lorenzani, C. Concari, G. Franceschini, and G. Buticchi, "Recent advances in single-phase transformerless photovoltaic inverters," *IET Renewable Power Gener.*, vol. 10, no. 2, pp. 260–273, 2016.
- [7] W. Yu et al., "High-efficiency inverter with H6-type configuration for photovoltaic non-isolated ac module applications," in *Proc. Annu. IEEE Appl. Power Electron. Conf. Expo.*, 2010, pp. 1056–1061.
- [8] B. Yang, W. Li, Y. Gu, W. Cui, and X. He, "Improved transformerless inverter with common-mode leakage current elimination for a photovoltaic grid connected power system," *IEEE Trans. Power Electron.*, vol. 27, no. 2, pp. 752–762, Feb. 2012.
- [9] F. Bradaschia, M. C. Cavalcanti, P. E. P. Ferraz, F. A. S. Neves, E. C. Santos, and J. H. G. M. da Silva, "Modulation for three-phase transformerless z-source inverter to reduce leakage currents in photovoltaic systems," *IEEE Trans. Ind. Electron.*, vol. 58, no. 12, pp. 5385–5395, Dec. 2011.
- [10] Y. Gu, W. Li, Y. Zhao, B. Yang, C. Li, and X. He, "Transformerless inverter with virtual dc bus concept for cost-effective grid-connected PV power systems," *IEEE Trans. Power Electron.*, vol. 28, no. 2, pp. 793–805, Feb. 2013.
- [11] W. Li, Y. Gu, H. Luo, W. Cui, X. He, and C. Xia, "Topology review and derivation methodology of single phase transformerless photovoltaic inverters for leakage current suppression," *IEEE Trans. Ind. Electron.*, vol. 62, no. 7, pp. 4537–4551, Jul. 2015.
- [12] H. Schmidt, C. Siedlke, and J. Ketterer, "DC/AC converter to convert direct electric voltage to alternating voltage or current," U.S. Patent 7 046 534 B2, May 16, 2006.
- [13] M. Islam and S. Mekhilef, "H6-type transformerless single-phase inverter for grid-tied photovoltaic system," *IET Power Electron.*, vol. 8, pp. 636–644, 2015.
- [14] W. Yu, J. Lai, H. Qian, and C. Hutchens, "High-efficiency MOSFET inverter with H6-type configuration for photovoltaic non isolated ac-module applications," *IEEE Trans. Power Electron.*, vol. 26, no. 4, pp. 1253–1260, Apr. 2011.
- [15] W. Cui, B. Yang, Y. Zhao, W. Li, and X. He, "A novel single-phase transformerless grid-connected inverter," in *Proc. 37th Annu. Conf. IEEE Ind. Electron. Soc.*, 2011, pp. 1067–1071.
- [16] M. Islam, N. Afrin, and S. Mekhilef, "Efficient single phase transformerless inverter for grid-tied PVG system with reactive power control," *IEEE Trans. Sustain. Energy*, vol. 7, no. 3, pp. 1205–1215, Jul. 2016.
- [17] M. Islam and S. Mekhilef, "Efficient transformerless MOSFET inverter for a grid-tied photovoltaic system," *IEEE Trans. Power Electron.*, vol. 31, no. 9, pp. 6305–6316, Sep. 2016.
- [18] N. Vázquez, M. Rosas, C. Hernández, E. Vázquez, and F. Perez, "A new common-mode transformerless photovoltaic inverter," *IEEE Trans. Ind. Electron.*, vol. 62, no. 10, pp. 6381–6391, Oct. 2015.
- [19] Wechselrichter, German Patent DE 19642522 C1, Apr. 23, 1998.
- [20] G. F. W. Khoo, R. H. Douglas, and R. A. McMahon, "Analysis of a charge pump power supply with a floating voltage reference," *IEEE Trans. Circuits Syst. I, Fundam. Theory Appl.*, vol. 47, no. 10, pp. 1494–1501, Oct. 2000.
- [21] F. Blaabjerg, R. Teodorescu, M. Liserre, and A. V. Timbus, "Overview of control and grid synchronization for distributed power generation systems," *IEEE Trans. Ind. Electron.*, vol. 53, no. 5, pp. 1398–1409, Oct. 2006.
- [22] W. L. Chen and J. S. Lin, "One-dimensional optimization for proportional resonant controller design against the change in source impedance and solar irradiation in PV systems," *IEEE Trans. Ind. Electron.*, vol. 61, no. 4, pp. 1845–1854, Apr. 2014.
- [23] M. Saitou and T. Shimizu, "Generalized theory of instantaneous active and reactive powers in single-phase circuits based on Hilbert transform," in *Proc. 33rd Annu. IEEE Power Electron. Spec. Conf.*, 2002, vol. 3, pp. 1419–1424.

- [24] Y. Yang, F. Blaabjerg, and H. Wang, "Low voltage ride-through of single-phase transformerless photovoltaic inverters," IEEE Trans. Ind. Appl., vol. 50, no. 3, pp. 1942–1952, May/Jun. 2014.
- [25] A. Timbus, M. Liserre, R. Teodorescu, P. Rodriguez, and F. Blaabjerg, "Evaluation of current controllers for distributed power generation systems," IEEE Trans. Power Electron., vol. 24, no. 3, pp. 654–664, Mar. 2009.
- [26] S. V. Araujo, P. Zacharias, and R. Mallwitz, "Highly efficient single-phase transformerless inverters for grid-connected photovoltaic systems," IEEE Trans. Ind. Electron., vol. 57, no. 9, pp. 3118–3128, Sep. 2010.
- [27] P. Channegowda and V. John, "Filter optimization for grid interactive voltage source inverters," IEEE Trans. Ind. Electron., vol. 57, no. 12, pp. 4106–4114, Dec. 2010.
- [28] A. G. Matias, F. Alejandro, L. Piotr, C. Tomasz, D. Valcan, and P. Alejandro, "Control of grid converter for wind turbines," Partial fulfillment of the requirements for M.S. degree, Aalborg Univ., Aalborg, Denmark, Groups PED-842, MCE2-830, 2009.
- [29] R. P. Alzola, M. Liserre, F. Blaabjerg, R. Sebastian, J. Dannehl, and F. W. Fuchs, "Analysis of the passive damping losses in LCL-filter-based grid converters," IEEE Trans. Power Electron., vol. 28, no. 6, pp. 2642–2646, Jun. 2013.
- [30] W. Wu, Y. He, T. Tang, and F. Blaabjerg, "A new design method for the passive damped LCL and LLCL filter-based single-phase grid-tied inverter," IEEE Trans. Ind. Electron., vol. 60, no. 10, pp. 4339–4350, Oct. 2013.

**AUTHORS DETAILS:**

**K. TEJA SREE**, received her B.TECH degree from KODADA INSTITUTE OF TECHNOLOGY AND SCIENCE FOR WOMEN, KODADA. Present she is pursuing M.TECH in VIDYA JYOTHI INSTITUTE OF TECHNOLOGY, Aziz Nagar, HYDERABAD.



**Mr. B. RAJESH**, is working as Assistant Professor in the department of Electrical and Electronics Engineering in Vidya Jyothi Institute of Technology. He is currently pursuing PhD from JNTUH Hyderabad. His areas of interest are Power Electronics controlled Drives and Power Electronics applications for Power systems.